



The Gel Point as Reference State: A Simple Kinetic Model for Crosslinking Polybutadiene via Hydrosilation

Michael E. De Rosa,^{a*} Marian Mours^b & H. Henning Winter^{a,b†}

^aDepartment of Polymer Science and Engineering, University of Massachusetts, Amherst, MA 01003, USA

^bDepartment of Chemical Engineering, University of Massachusetts, Amherst, MA 01003, USA

(Received 20 April 1996; accepted 25 July 1996)

ABSTRACT

Kinetic data can be described in a simple model when using the gel point as reference state. This has been shown for crosslinking data on five high molecular weight polybutadienes (18 100–97 000 g/mol). Experiments were carried out under isothermal conditions with a constant amount of catalyst. Crosslinking took place by a hydrosilation reaction at vinyl sites which were randomly distributed along the backbone of the polybutadiene precursor molecules using the bifunctional aromatic silane p-bis(dimethylsilyl) benzene as connector. FTIR measurements showed that the hydrosilation reaction followed first order kinetics. The critical gel time, t_c , was determined by the instant at which power law relaxation behavior was observed (i.e. $\tan \delta = \text{constant}$) over the two lowest decades in frequency. The main parameters that were observed to affect t_c were the stoichiometric ratio, r , and the functionality of the polybutadiene, f . It was observed that the time to reach the gel point decreased with increasing precursor molecular weight ($\sim f$) of the polybutadiene. The gel time also decreased when increasing the initial amount of silane crosslinker. We were able to find a relationship between the gel time measured by the CFS technique and r and f by coupling the Flory–Stockmayer gelation theory with a simple first order kinetic curing scheme. © 1997 Published by Elsevier Science Limited. All rights reserved

1 INTRODUCTION

Crosslinking polymer molecules are able to chemically connect into large clusters which grow with conversion, p , of the reactive sites. At a critical

* Present address: Wright Laboratory Materials Directorate WL/MLPJ, Wright Patterson Air Force Base, OH 45433, USA.

† Author to whom correspondence should be addressed.

conversion, p_c , the polymer undergoes a liquid–solid transition. The instant of this transition is called the critical gel point. Engineers wishing to process crosslinking polymers or develop specific materials with desired mechanical properties near the gel point find that it is crucial to determine the time to reach the gel point, t_c , so that processes can be tailored in this region.

Rheological methods present the most effective and practical way to monitor the evolution of network structure during gelation. Common techniques include measuring the steady shear viscosity^{1–6} or dynamic mechanical shear properties^{7–14} as a function of reaction time and frequency. Other methods based on more qualitative observations have also been reported, e.g. the hot plate and spatula method¹⁵ or the indentation of the surface of the crosslinking polymer with a thumb and subsequent observation as to whether this indentation vanishes.¹⁶

Rheology is able to identify the gel point since stress relaxation at t_c is characterized by a power law pattern. The power law is a manifestation of the critical self-similar structure of the gel. The shear relaxation modulus was found to be^{8,17,18}

$$G(t) = St^{-n} \quad \text{for } \lambda_0 < t < \infty \quad (1)$$

where S is the gel stiffness and n is the critical exponent which takes on values $0 < n < 1$. λ_0 is the shortest time for the self-similar relaxation which is characteristic for the crossover to a new relaxation regime at shorter times.

The corresponding complex modulus has the form

$$G^*(\omega) = \Gamma(1 - n)S(i\omega)^n \quad \text{for } 0 < \omega < 1/\lambda_0 \quad (2)$$

The advantage of using dynamic mechanical techniques is that the sample can be probed from the liquid to the solid state through the critical gel point while remaining in the linear viscoelastic region without disrupting the developing structure. In our study we use one such technique called time-resolved rheometry.¹⁹ The material is probed by cyclic frequency sweeps (CFS) which are ideally suited for gelation studies because they give an accurate measurement of the gel time which is the parameter of most interest in this investigation, and, additionally, provides data to quantify the parameters S and n and the rate of change of the dynamic shear properties near the gel point.

The gel time depends upon a variety of system dependent experimental parameters such as temperature, catalyst concentration, inhibitor concentration, and/or radiation dosage. Specifically important parameters for

chemical gelation are the stoichiometric ratio, r , and the functionality, f , of the precursor molecules. As an example, Arellano *et al.*¹⁵ found for an epoxy system during cure that increasing r (defined as the number of functional groups of the epoxy molecule divided by the number of functional groups of the amine molecule) caused the gel time to increase.

In this study we investigated the kinetics of crosslinking of polybutadiene precursors via hydrosilation. Our objective was to distinguish the molecular parameters which strongly influence the gelation behavior and especially the gel time. The gel times of polybutadienes of various functionalities, f , crosslinked with a bifunctional crosslinker in numerous stoichiometric ratios, r , were measured. We wanted to find a simple correlation between the measured gel times and the parameters f and r that allows us to predict t_c as a function of the precursor composition by incorporating a simple kinetic curing scheme with the branching theory predictions of p_c given by Flory^{20,21} and Stockmayer.²² It was shown by other researchers^{23,24} that this mean field prediction of p_c agrees reasonably well with experimental data. Mean field theory predicts the infinite cluster at the gel point and the time to obtain it; however, in general it does not describe the material structure properly due to the non-physical nature of the underlying Bethe lattice. Percolation theory²⁵ is more useful to predict the proper connectivity. A similar approach was taken by Batch *et al.*¹⁶ to calculate the gel times of crosslinking polydimethylsiloxanes. However, their method of gel point determination only allowed a very crude estimate of the gel time.

2 EXPERIMENTAL

2.1 Materials and characterization

Five polybutadienes of different molecular weight and narrow molecular weight distribution were synthesized by Dr Michael Masse (Shell Development Co.) using a standard anionic polymerization technique. The details of the synthesis are described in a previous paper on the relaxation behavior of the uncrosslinked polybutadiene polymers.²⁶ The molecular weights and polydispersities were measured by gel permeation chromatography. The 1,2-vinyl content was determined by proton NMR and the relative *cis* and *trans* content along the chain backbone by FT Raman spectroscopy on a Bruker instrument model IFS-88 with FT Raman

TABLE 1
Characterization summary of polybutadiene precursor polymers

Sample	M_w	M_w/M_n	% cis	% trans	% vinyl	Average functionality, f	T_g (°C)
PBD18	18 100	1.03	41	52	7.30	23.8	-92
PBD20	20 700	1.04	39	53	8.19	30.2	-91
PBD38	37 900	1.05	41	51	7.70	51.5	-92
PBD44	44 100	1.04	39	53	8.11	63.7	-90
PBD70	70 200	1.02	43	50	7.30	93.0	-93
PBD97	97 000	1.07	41	51	8.04	135.0	-90

module FRA 106 attachment. Glass transition temperatures were obtained on a DuPont DSC instrument model 2910 at a heating rate of 20 K/min. A summary of the characterization results is given in Table 1.

2.2 Crosslinking reaction

The polybutadiene chains were crosslinked at the 1,2-vinyl sites along their backbone with an aromatic bifunctional silane crosslinker, *p*-bis(dimethylsilyl) benzene. The reaction is catalyzed by *cis*-dichlorobis(diethylsulfide) platinum(II) which was dissolved in toluene. Details of the reaction have been given elsewhere.^{27,28}

Crosslinker and precursor were mixed at desired stoichiometric ratios r (r = moles of SiH/moles of vinyl). Due to the narrow molecular weight distribution, the accurately measured vinyl content of the polybutadiene prepolymer and the specificity of the hydrosilation reaction between the vinyl group and SiH group of the crosslinker, we are able to define the prepolymer functionality of the polybutadienes as the average number of reactive vinyl sites per precursor chain. This was evaluated as²⁹

$$f = P_{\text{vinyl}} \overline{X}_n \quad (3)$$

where P_{vinyl} is the percentage of total butadiene monomer units in the chain that are vinyl units as measured by ¹H NMR. \overline{X}_n is the number average degree of polymerization of the precursor molecules and is calculated as³⁰

$$\overline{X}_n = \frac{M_n}{M_0} \quad (4)$$

where M_0 is the molecular weight of the butadiene monomer (54 g/mol) and M_n is the number average molecular weight of the polymer. At constant vinyl content, the functionality of the prepolymer increases directly with the precursor molecular weight. The spacing of the vinyl group along the backbone is assumed to be random.

Other researchers³¹ have demonstrated that it is actually more appropriate for polydisperse material to define the functionality based on the weight average degree of polymerization rather than the number average as proposed by Friedmann and Brossas.²⁹ For the current study, however, the difference in f is negligible due to the near monodispersity of the precursor polymers.

2.3 Sample preparation

Samples were prepared by mixing 0.6 g of polybutadiene with 0.06 ml (350 ppm) of catalyst solution in toluene (8.0×10^{-3} mol/l) for 10–12 min with a microspatula in a ceramic crucible. The mixing process is very effective since the sample was ‘folded’ with every move of the spatula, e.g. folding the sample 20 times increases the number of ‘layers’ within the sample by a factor of approximately 10^6 . The toluene introduced by the catalyst solution (approximately 8 wt%) was removed by vacuum stripping the mixture at 70°C for 2 h. Afterwards, the sample was allowed to cool to room temperature. The desired amount of crosslinker (purity > 99.5%) was added with a 0.1 ml Hamilton syringe and mixed in at ambient conditions for 6 min. This addition of crosslinker initiated the reaction. Samples were then loaded in between preheated rheometer fixtures and cured at 28, 34, and 40°C.

Cure temperatures in the rheometer were controlled to within ± 0.5 K. A time of 1.5 min was required to load the sample and start the measurement. A total time of 7.5 min was used for mixing and loading for the cure cycles at 34 and 40°C and 10 min for 28°C. At the end of the mixing and loading time, the rheological measurement was started.

Since temperature affects the rate of reaction, the room temperature is important to take into consideration during the mixing phase. To minimize this effect, experiments were performed over a period of time in which the room temperature did not vary significantly. For samples cured at 34 and 40°C, the room temperature was $25.5 \pm 1.5^\circ\text{C}$. For samples cured at 28°C, the room temperature was $21.5 \pm 1.5^\circ\text{C}$. Gel time data were not accepted for experiments which were prepared at room temperatures outside this 1.5 K temperature tolerance.

The reproducibility of the gel point was very good despite the small

amount of sample used for each experiment. Gel times for different samples with the same stoichiometry usually agreed to within 1–2 min.

2.4 Rheological measurements

Dynamic mechanical measurements were performed in a Rheometrics RDS 7700 with 25 mm parallel disk fixtures. Heated nitrogen was circulated throughout the environment chamber for measurements performed at 34 and 40°C while air was used for the experiments at 28°C.

The gel times of the crosslinking materials were measured with the technique of cyclic frequency sweeps (CFS).^{13,28,32,33} This method studies the evolving structure of the material by probing it with consecutive frequency sweeps which results in time and frequency dependent data. Each data point represents a different state of the network and interpolation is needed to evaluate the dynamic moduli over the entire frequency window at a specific extent of reaction. Data in the vicinity of the gel point were therefore interpolated with the computer program GELPRO.¹⁹

The critical gel time was easily determined by the self-similar relaxation pattern at the gel point (i.e. $\tan \delta$ is constant over the terminal frequency range). An example of the gel point determined by CFS is given in Fig. 1.

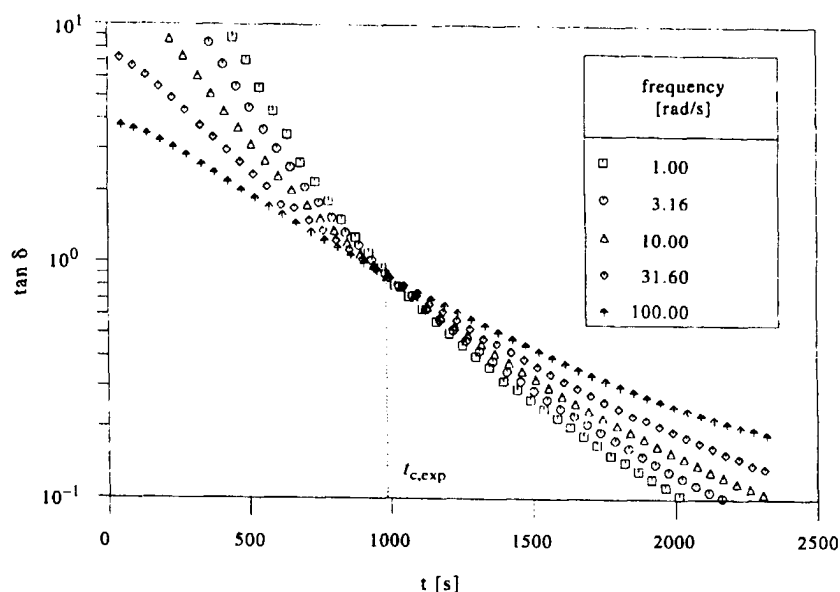


Fig. 1. CFS data showing the evolution of $\tan \delta$ during crosslinking for PBD38 ($r = 1$) at 28°C as a function of the experimental time, t_{exp} . The frequency range from 1 to 100 rad/s is shown. $t_{\text{c,exp}}$ indicates the critical gel time.

The intersection of the $\tan \delta$ curves over the frequency window gives the time of gelation.

We propose to use the gel point (and the associated properties of the critical gel) as reference state when analysing the experimental data. This has several advantages:

- the gel point lies in the middle of the most interesting region of the experiment;
- the gel point can be measured;
- the critical gel properties n , S , and λ_0 can be measured;
- a controlled environment has been established.

The conventional representation of the data has been with respect to the initial conditions. However, these initial conditions are quite ill-defined since the reacting sample is being subjected to two different environments. The first is the ambient condition of the room during the time it takes to mix the precursor, catalyst, and crosslinker and load them into the rheometer. During this initial mixing and loading stage, the sample is reacting. Therefore, the extent of reaction at the beginning of the kinetic CFS measurement is not zero (and it is ill-defined). The CFS measurement on the reacting sample begins at the experimental time $t_{\text{exp}} = 0$ when the reaction has already proceeded to some (yet unknown) initial extent of reaction $p = p_i$. A controlled environment, i.e. controlled temperature of the chamber of the rheometer, can only be provided for the second and main part of the experiment. These are the reasons for the above procedure in which we use $(t_c - t)$ as time scale and not t by itself.

The initial extent of reaction cannot be easily reduced. One could envision a modified sample preparation with less catalyst to decrease the reaction rate and thereby reduce p_i . This however results in very long experimental times which are not necessarily practical. An increase in temperature for the CFS experiment to compensate for the catalyst reduction is not advisable since the importance of side reactions increases with increasing temperatures.³⁴

The clock might be started at three different times. One may describe the experiment with: (1) the actual reaction time, t_{react} , that includes the sample's actual temperature history; (2) the time of the rheological experiment, t_{exp} , at T_{exp} ; or (3) a time $t_{\text{exp}} + \Delta t_i$ for the hypothetical case that the entire experiment including mixing and loading was carried out at T_{exp} . The time of gelation measured by CFS is given a value $t_{c,\text{exp}}$. It differs by Δt_i from the real gel time at the reaction temperature, t_c . A schematic representation of the cure cycle of the kinetic experiment and the different time scales involved is given in Fig. 2.

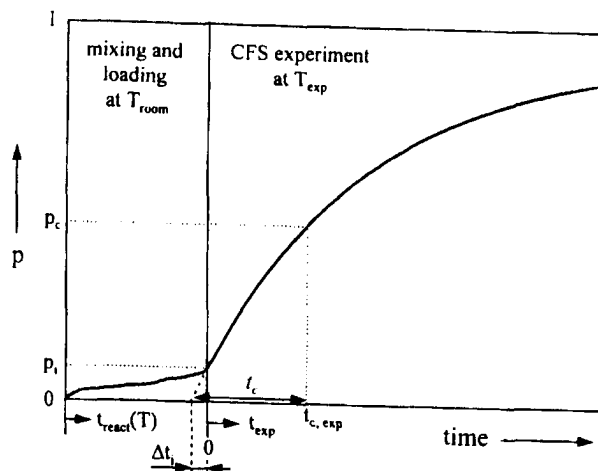


Fig. 2. Schematic representation of the kinetic experiment showing the extent of reaction, p , versus reaction time, t_{react} . After mixing and loading at T_{room} the CFS measurement is performed at T_{exp} in the rheometer. At the beginning of the CFS experiment the extent of reaction has reached a value of p_1 and a new time scale, $t_{\text{c,exp}}$, begins. $t_{\text{react}}(T_{\text{exp}})$ denotes the reaction time for the hypothetical case that the entire experiment had been performed at T_{exp} .

2.5 FTIR measurements

FTIR spectroscopy was used to measure the curing kinetics, $p(t)$, of PBD18 in order to find the reaction order of the hydrosilation. Measurements were made on an IBM 98 Fourier transform infrared spectrometer. Data was analysed with LabCalc software (Galactic Industries Corp.). Samples were prepared in the same way as for CFS measurements. After mixing for 6 min, the reacting mixture was loaded between polished KBr plates and then placed in the sample compartment which was purged of H_2O vapor and CO_2 with dry air. The measurement was carried out at the temperature of the sample compartment which was measured to be $25 \pm 1^\circ\text{C}$. It was not necessary to perform the FTIR experiments at the same reaction temperature as the rheological experiments since the reaction order is not expected to change dramatically within a few degrees. No direct correlation between rheological experiment and extent of reaction data from FTIR was attempted in this study. Data were collected manually and stored in units of absorbance approximately every 3–5 min for the first hour and every 7–10 min for the next hour. Each spectrum represents an average of 32 scans which required 20 s. The recorded time of the measurement was taken at the 16th scan. The amount of chemical change that took place during a single measurement (32 scans) was negligible and will not cause significant error.

Data that were taken early on in the reaction had interference from the absorbance of water vapor and carbon dioxide since not all of the moisture and CO₂ (moisture and CO₂ entered the FTIR cell during sample loading) was completely purged at the time of initial measurements. These peaks (mostly between 1450–1750 cm⁻¹ and 2300–2400 cm⁻¹) were later subtracted from the spectra using LabCalc.

3 RESULTS

3.1 CFS values of the gel times

To determine the effect that the stoichiometric ratio and the functionality of the chain had on the measured gel times, experiments were run using a variety of precursor compositions at three different temperatures. The values of the CFS gel times are given in Table 2 for cure temperatures of 28, 34, and 40°C.

3.2 Effect of stoichiometric ratio on the measured gel time

The precursor composition significantly influences the gel time as measured by the CFS technique. The first observation was the strong

TABLE 2
Gel times measured by CFS ($t_{c,exp}$) as defined in Figure 2

Sample	r	$t_{c,exp}$ (s) at 28°C	$t_{c,exp}$ (s) at 34°C	$t_{c,exp}$ (s) at 40°C
PBD18	0.09			3070
	0.122			2140
	0.175			1750
	0.404			876
PBD38	0.1		5090	
	0.124			1170
	0.15		3200	
	0.25	2560	2300	
	1.0	958		
	1.39		670	
	2.0	580		
PBD44	0.25	2140	1140	
	0.5	1240	750	
	0.8		450	
PBD70	0.5	845		
PBD97	0.5	820		

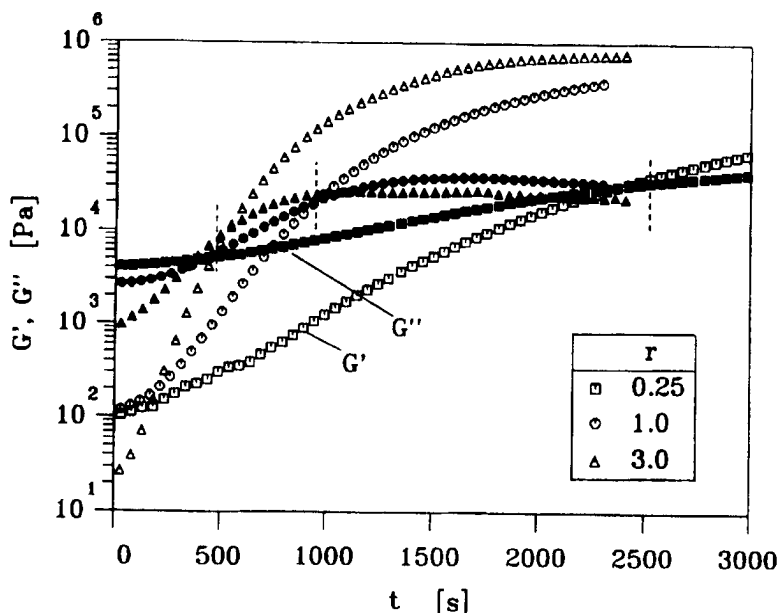


Fig. 3. Evolution of the dynamic moduli as a function of t_{exp} at 3.16 rad/s during gelation for PBD38 at 28°C for three stoichiometric ratios r . Filled symbols represent G' , open symbols represent G'' . The approximate gel times, $t_{\text{c,exp}}$, are indicated by the dashed lines.

dependence of the gel time on the stoichiometric ratio. Figure 3 shows the evolution of the dynamic moduli at 3.16 rad/s for PBD38 at $r = 0.25$, 1.0, and 3.0 cured at 28°C. The values of the critical relaxation exponent n for these samples are 0.45, 0.45, and 0.47, respectively. The dashed lines are used to indicate the approximate gel time. It can be seen that, as the silane content was increased from $r = 0.25$ to 3.0, the gel time decreased dramatically. Such a trend was observed for all precursor molecular weights.

3.3 Effect of functionality on the measured gel time

Another parameter which strongly influences the gel time is the functionality of the precursor molecule. Figure 4 shows the evolution of the dynamic moduli during crosslinking at 3.16 rad/s for samples PBD18, PBD38, and PBD70 cured at 28°C with balanced stoichiometry ($r = 1.0$). The dashed lines again mark the gel point. From the data it is evident that, as the average functionality of the precursor sample is increased from 23.8 to 93.0, the value of the gel time decreases.

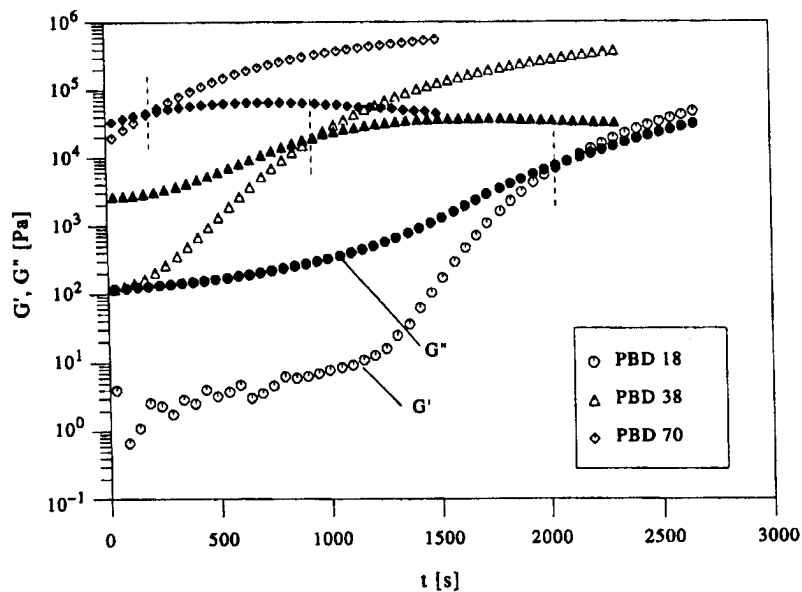


Fig. 4. Evolution of the dynamic moduli as a function of $t_{c,exp}$ at 3.16 rad/s during gelation at balanced stoichiometry ($r = 1$) for three precursor molecular weights. Filled symbols represent G' , open symbols represent G'' . The approximate gel times, $t_{c,exp}$, are indicated by the dashed lines.

3.4 FTIR measurements

The kinetics of the crosslinking reaction of PBD18 with stoichiometric ratios of 1.0 and 0.5 was monitored using FTIR spectroscopy. This was done by measuring the intensity of the silane (SiH) absorption band which appears as a well isolated peak at 2116 cm^{-1} . There is no interference by any other absorption band from other bonds in the crosslinker molecule or the polybutadiene. FTIR has been used extensively to monitor the evolution of silane conversion during hydrosilation.^{10,35-38} FTIR data in Fig. 5 show the decrease in the silane peak during the crosslinking of sample PBD18.

A calibration curve for verifying Beer's law³⁹ was measured with four mixtures of crosslinker and PBD18 with stoichiometric ratios of $r = 0.25$, 0.5, 0.75, and 1.0. The measured silane peak heights at 2116 cm^{-1} were normalized with a reference peak at 1436 cm^{-1} (CH_3/CH_2 deformation peak). The peak at 1436 cm^{-1} was chosen as an internal standard because its peak height changed by less than 5% during the reaction. Use of an internal standard peak eliminates factors that can affect the absorption intensity, such as sample thickness. Figure 6 shows the plot of normalized

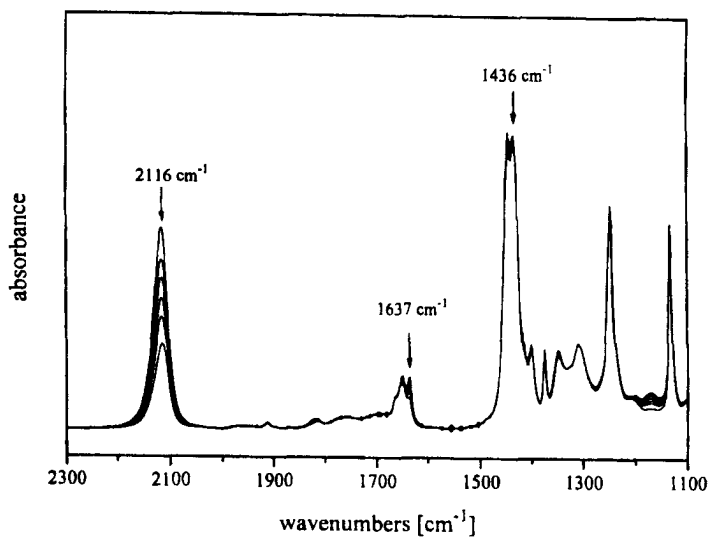


Fig. 5. FTIR kinetic data at $25 \pm 1^\circ\text{C}$ showing the conversion of silane at 2116 cm^{-1} during crosslinking of PBD18 with stoichiometric amount of silane ($r = 1$). The peak at 1436 cm^{-1} was used as internal reference.

silane peak heights versus r . The linear dependence signifies that Beer's law holds and therefore the concentration of silane is directly proportional to the normalized silane peak heights.

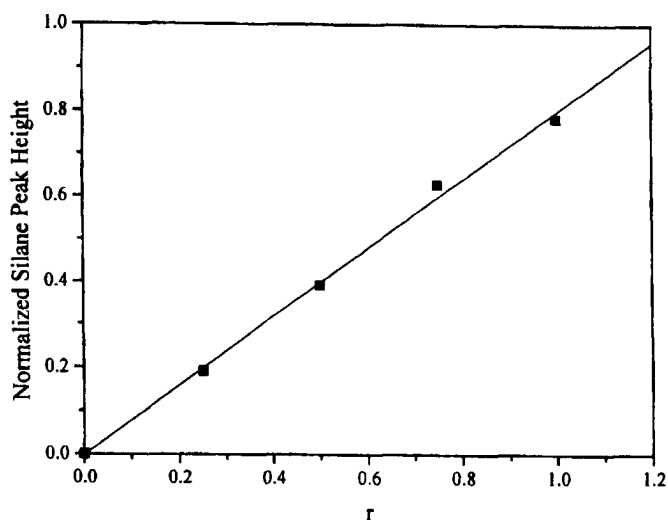


Fig. 6. FTIR calibration curve showing the linear dependence of the normalized silane peak intensity versus stoichiometric ratio.

The extent of reaction, p , was calculated by

$$p(t) = \frac{R(0) - R(t)}{R(0)} \quad (5)$$

where $R(t)$ is the normalized silane peak intensity ratio at time t and $R(0)$ is the normalized peak intensity ratio at reaction time $t_{\text{react}} = 0$. This is equivalent to

$$p(t) = \frac{[\text{SiH}]_0 - [\text{SiH}]_t}{[\text{SiH}]_0} \quad (6)$$

where $[\text{SiH}]_0$ is the initial concentration of silane (at $t_{\text{react}} = 0$) and $[\text{SiH}]_t$ is the concentration of silane at some time t during the reaction. The extent of reaction versus reaction time, $t_{\text{react}}(T)$ (see Fig. 2), for stoichiometric ratios of 1.0 and 0.5 is shown in Fig. 7.

4 ANALYSIS

We first determine the order of the reaction since this affects the entire analysis. Then we integrate the rate equation for p and introduce the gel

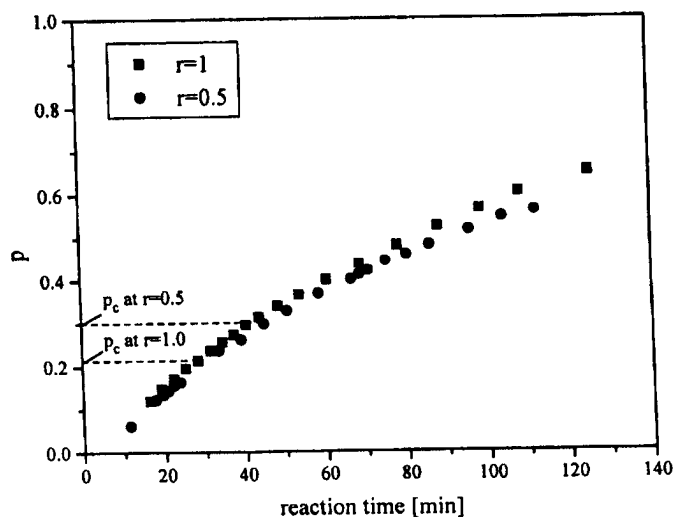


Fig. 7. Extent of reaction of silane, p , as calculated from the FTIR data at $25 \pm 1^\circ\text{C}$, is plotted versus reaction time (t_{react}) for two initial compositions of PBD18 and crosslinker ($r = 0.5$ and 1). The values of the critical extents of reaction, p_c , calculated by branching theory, are given for both initial compositions.

point as reference state. Approximation of p_c with the Flory–Stockmayer model leads to a simple relation for $p(t)$ with parameters r , f , and T .

4.1 Order of reaction

If we assume that the reaction between the SiH unit and the vinyl unit follows the mechanism proposed by Chalk and Harrod,³⁵ then we can describe the kinetics in the same manner as reported by Macosko and Lee⁴ for the hydrosilation crosslinking of polydimethylsiloxane. The consumption of silane can be described by

$$-\frac{d[\text{SiH}]}{dt} = k[\text{Pt}][\text{SiH}]^m \quad (7)$$

where m is the reaction order, $[\text{Pt}]$ is the platinum concentration and k is the rate constant. Equation (7) can be simplified if it is realistic to assume that $[\text{Pt}]$ remains nearly constant during the reaction:

$$-\frac{d[\text{SiH}]}{dt} = \bar{k}[\text{SiH}]^m \quad (8)$$

with $\bar{k} = k[\text{Pt}]$.

For integrating eqn (8), we need a reference state which ideally would be the initial state at $t_{\text{react}} = 0$ and $[\text{SiH}]_0$ as prescribed by the composition of the sample. However, during the initial period of the sample preparation, the reaction path is somewhat complicated by the mixing kinematics and the temperature history. We therefore propose to take the critical gel as reference. It has the advantage of knowing t_c (from rheology) and $[\text{SiH}]_c$ (from FTIR) and the reaction parameter \bar{k} can be assumed to be a constant in the vicinity of the gel point. To simplify matters, we assume the reaction can take on three possible values of m . If eqn (8) is integrated with limits $[\text{SiH}]$ to $[\text{SiH}]_c$ at times from t to t_c , respectively, for a reaction order of 1, 1.5, and 2 the results are

$$\text{for } m = 1: [\text{SiH}] = [\text{SiH}]_c e^{-\bar{k}(t-t_c)} \quad (9)$$

$$\text{for } m = 1.5: \frac{1}{\sqrt{[\text{SiH}]}} = \frac{1}{\sqrt{[\text{SiH}]_c}} + \frac{1}{2} \bar{k}(t - t_c) \quad (10)$$

$$\text{for } m = 2: \frac{1}{[\text{SiH}]} = \frac{1}{[\text{SiH}]_c} + \bar{k}(t - t_c) \quad (11)$$

Linear plots of $\ln [\text{SiH}]$ versus t , $1/\sqrt{[\text{SiH}]}$ versus t , and $1/[\text{SiH}]$ versus t from FTIR data are able to provide evidence as to whether the reaction

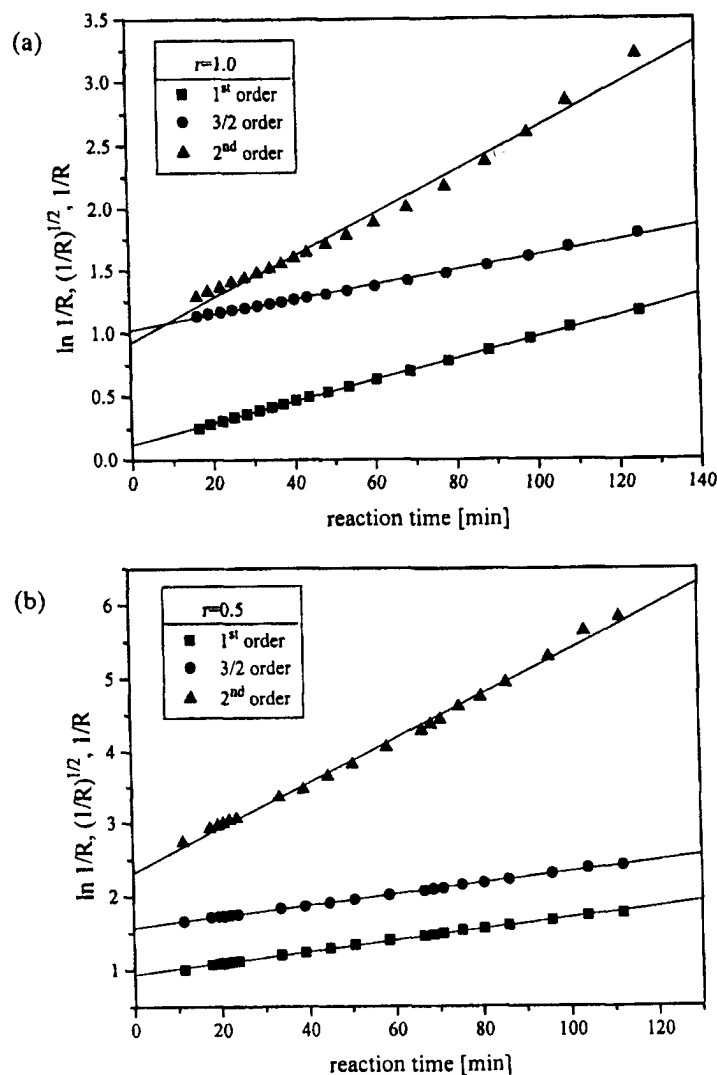


Fig. 8. FTIR kinetic data plotted for the determination of the reaction order. R is the normalized silane peak height ratio which is directly proportional to silane concentration. Data is plotted for the initial concentration of (a) $r = 1$ and (b) $r = 0.5$.

is of order 1, 1.5, or 2, respectively.⁴⁰ The silane concentrations are plotted in terms of normalized absorbance intensities. Figure 8 shows plots of FTIR kinetic data of curing PBD18 at $r = 1.0$ and 0.5 . For $r = 0.5$ it appears that the reaction rate could be described as either of order 1 or 1.5. For $r = 1.0$, the data are best described by a first order plot. Soltero and Gonzalez-Romero⁴¹ who studied a polydimethylsiloxane network

system also found that a first order kinetic scheme fitted reasonably well for the hydrosilation reaction. Therefore, we will use first order kinetics in our model.

4.2 Flory–Stockmayer prediction of p_c

The qualitative trend in the value of t_c with the stoichiometry and the functionality of the precursor may be described with the branching theory of Flory^{20,21} and Stockmayer.²²

For the crosslinking of a multi-functional precursor with a bi-functional crosslinker, the Flory–Stockmayer branching theory predicts the critical extent of reaction of silane, $p_{c,\text{SiH}}$, needed to reach the gel point as a function of stoichiometry, r , and functionality of the polybutadiene, f , as

$$P_{c,\text{SiH}} = \frac{1}{\sqrt{r(f-1)}} \quad (12)$$

For the two cases examined, eqn (12) can be used to describe the experimentally observed trend in the gel times.

4.2.1 Case 1: variable r , constant f

For the first case, the functionality is kept constant and the stoichiometric ratio is changed. From eqn (12), $p_{c,\text{SiH}}$ decreases as r is increased by increasing the amount of crosslinker. Therefore, if the other factors that could influence the rate of the chemical crosslinking reaction are kept constant, such as the amount of catalyst and the temperature, $t_{c,\text{exp}}$ should occur at shorter times as r is increased, as seen in Fig. 3.

4.2.2 Case 2: variable f , constant r

In the second case, the stoichiometric ratio is kept constant and the functionality is increased by increasing the precursor molecular weight. From eqn (12), $p_{c,\text{SiH}}$ decreases if f is increased and r is kept constant. Therefore, by the same argument made for case 1, $t_{c,\text{exp}}$ would be expected to decrease as f increases as seen in Fig. 4. Arellano *et al.*¹⁵ examined the kinetics of a crosslinking epoxy system and they observed similar trends in the gel times as a function of stoichiometry and functionality.

4.3 Correlation between gel time and precursor composition (first order kinetics)

Classical branching theory can be used to qualitatively account for the observed trend in the gel time as a function of f and r . Although this finding is quite useful, it currently lacks the ability to quantitatively

predict the gel time as a function of these two parameters. The results will now be expanded by combining branching theory with simple kinetics to derive an empirical model to accomplish this goal.

Knowing that the hydrosilation reaction can be described as first order, eqn (9) can be used in the following gel time analysis. To make the connection between critical conversion of silane (eqn (12)) and the reaction rate, eqn (8) has to be expressed in terms of conversion, p , instead of concentration of silane. One substitutes eqn (6) into eqn (8) ($m = 1$) to obtain

$$\frac{dp}{dt} = \bar{k}(1 - p) \quad (13)$$

Integrating eqn (13) with the gel point as reference state results in

$$(1 - p) = (1 - p_c)e^{-\bar{k}(t-t_c)} \quad (14)$$

The critical extent of reaction might be approximated by the Flory-Stockmayer expression (eqn (12)) and the extent of reaction for SiH becomes

$$p = 1 - \left(1 - \frac{1}{\sqrt{r(f-1)}}\right)e^{-\bar{k}(t-t_c)} \quad (15)$$

with constant $\bar{k}(T) = k(T)[Pt]$ for variable T .

Alternatively, the reaction time can be expressed explicitly as

$$t_c - t = -\frac{1}{\bar{k}} \left[\ln \left(1 - \frac{1}{\sqrt{r(f-1)}}\right) - \ln(1 - p) \right] \quad (16)$$

The model might be refined by more accurate descriptions of p_c of more recent theories which could, for example, include side reactions.

A similar expression as in eqn (16) results when using the extent of reaction in terms of vinyl group concentration instead of in terms of silane group concentration. p_{SiH} and $p_{c,\text{SiH}}$ can be replaced by p_{vinyl}/r and $p_{c,\text{vinyl}}/r$. This does not change the general form of the kinetic equation.

4.4 Evaluation of kinetic parameters

The parameters of eqn (16) were evaluated by analysing the results of CFS kinetic data taken at three temperatures. CFS gel time ($t_{c,\text{exp}}$) plotted versus $\ln(1 - 1/\sqrt{r(f-1)})$ yields a linear relationship as seen in Fig. 9.

The slope gives the rate constant as $-\frac{1}{\bar{k}}$. The intercept with the abscissa at $t_{c,\text{exp}} = 0$ gives the extent of reaction at the end of the mixing and loading time p_i as $\ln(1 - p_i)$. An average value of $p_i = 0.0748$ is calculated

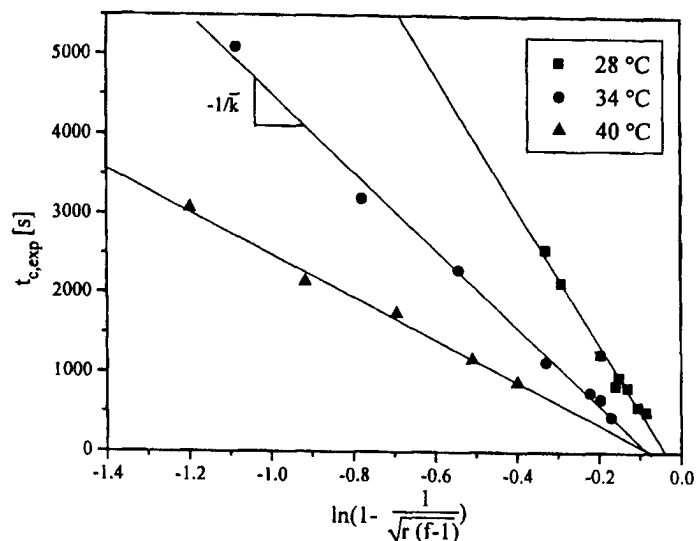


Fig. 9. Experimental gel times by CFS ($t_{c,exp}$) plotted versus a function of p_c (eqn (16)). p_c is calculated from eqn (12). Data is plotted for three temperatures. The slope of the plot gives the rate constant as $-1/\bar{k}$.

from the data sets at 34 and 40°C since the mixing and loading for those samples was carried out at the same room temperature (see Fig. 9, the intercept for the 34 and 40°C data sets is almost identical). Note, that the FTIR extent of reaction data is no longer used in this evaluation. The only experimental data needed to evaluate the rate constant are the gel time, t_c , the stoichiometric ratio, r , and functionality of the precursor, f .

The dependence of the rate constant on the cure temperature seems to follow an Arrhenius relationship⁴⁰

$$\bar{k} = Ae^{-E_a/RT} \quad (17)$$

where E_a is the activation energy of the reaction and A is the pre-exponential or frequency factor. Values of \bar{k} are given in Table 3. A

TABLE 3
Rate constants evaluated from kinetic data (all samples)

T (°C)	\bar{k} (s ⁻¹)
28.0	1.18×10^{-4}
34.0	2.04×10^{-4}
40.0	3.64×10^{-4}

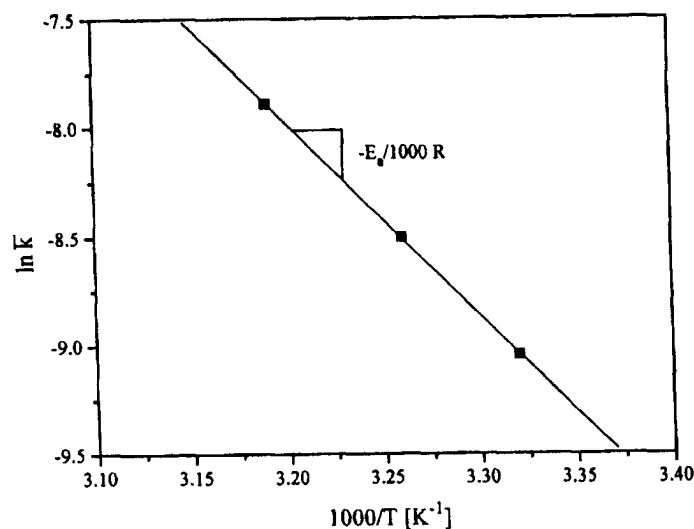


Fig. 10. Plot of rate constant \bar{k} (in s^{-1}) versus cure temperature. The slope yields the activation energy as $-E_a/1000R$.

plot of $\ln \bar{k}$ versus $1000/T$ yields a slope of $-E_a/1000R = -8.856 \text{ K}$ from which the activation energy of 74 kJ/mol is calculated (Fig. 10). With this activation energy the gel time for any precursor composition at any temperature can be calculated. All parameters of the kinetic model are given in Table 4.

4.5 Comparison of predicted gel time to experimental results

To test predictions with the measured gel time at different cure temperatures, three compositions of PBD18 were prepared for crosslinking. The room temperature for all three samples for the mixing and loading stage

TABLE 4
Parameters of gel time kinetic model

E_a/R (K)	8856
E_a (kJ/mol)	74
A (s^{-1})	6.95×10^8
p_1	0.0748

TABLE 5
Experimental CFS gel times compared to predicted gel times at three temperatures using the kinetic model with parameters from Table 4

T (°C)	r	Predicted gel time (s)	Experimental gel time (s)	% Difference
26.0	0.50	2870	3210 ± 30	+12
31.0	0.24	3100	3510 ± 30	+13
37.5	0.11	3230	3530 ± 50	+10

were at $25.5 \pm 1.0^\circ\text{C}$. The predicted gel times and experimental gel times are given in Table 5.

5 APPLICATION OF $p(t)$ EQUATION

The relationship between extent of reaction and time, eqn (15), has an important application in the rheometry of crosslinking materials. The time t or $|t - t_c|$ is the measurable variable in a rheological experiment while the chemical extent of reaction, p , characterizes the actual state of the material. Therefore, the extent of reaction, p , or the distance from the gel point, $|p - p_c|$, is used in gelation theories to describe the progress of reaction. Equation (15) can be easily used to convert the experimental accessible parameter, $|t - t_c|$, to the more useful $|p - p_c|$. Very near the gel point, eqn (15) can be linearized. The material functions then show the same functional behavior with $|p - p_c|$ and $|t - t_c|$, only the front factors differ. The range of validity of such a linearization, however, highly depends on the functional form of the $p(t)$ relationship.

For our material, simple first order kinetics govern the reaction. Nevertheless, the preceding arguments are valid also for different order kinetics. The equivalent relationships which replace the first order kinetics equations (eqns (15) and (16)) are given in the Appendix.

6 DISCUSSION

The relationship given by eqn (16) agrees with the measured experimental gel times to within 10–13%. The experimental gel times are generally larger than the predicted ones which can be attributed to the occurrence of side reactions such as ring formation. Such side reactions consume crosslinker but do not contribute to the network. By using the Flory–Stockmayer expression for the critical conversion, p_c , we cannot include

the influence of those side reactions since their model does not account for side reactions.

Our model is rather sensitive to the input parameters. The greatest source of deviation originates from errors introduced in evaluating E_a/R and the average value of p_i . Experimental data at three temperatures were used to evaluate E_a/R . Usually, more data sets at several different temperatures are needed to obtain a more accurate value of the activation energy. Furthermore, only two values of p_i were used to calculate an average p_i resulting in a significant uncertainty. Measuring more gel times at different curing temperatures is necessary to achieve more precise values for these input parameters.

The effects of temperature gradients were not taken into account in this model. Temperature gradients across the thickness of the sample, from the plate-sample interface to the center of the sample, produce gradients in the extent of reaction, and consequently the mechanical properties are functions of the sample thickness. Temperature gradients were reduced by using cure temperatures that were less than 15 K above ambient conditions and by using samples with minimum thickness (≈ 0.5 mm). Use of higher cure temperatures with greater sample thickness would increase the potential for inhomogeneity in samples. Models have been developed to predict temperature gradient effects and their relationship to gradients in extent of reaction and mechanical properties as a function of sample thickness.^{4,16}

Our observations focused on two independent ways of affecting the rate of change of mechanical properties: (1) the rate of the hydrosilation reaction; and (2) the precursor composition. In the first case, the rate of the chemical reaction has been increased by increasing the temperature or the amount of catalyst used. When silane bonds are converted at a faster rate, this causes crosslinks to be formed at a faster rate. The result is an increase in the rate of evolution of the dynamic mechanical shear properties and thus shorter gel times.

However, in this study we kept the temperature and amount of catalyst constant and still observed a dramatic change in the gel times while only varying the precursor composition. This could be qualitatively described for two cases by using the Flory-Stockmayer prediction. The first case involved changing the initial concentration of silane and keeping the functionality constant. Taking into account the fact that the reaction was first order, the rate of conversion of silane and therefore $p(t)$ should be independent of the initial concentration of silane as given by eqn (13) and shown experimentally by the FTIR data (Fig. 7). Therefore, temperature or catalyst concentration cannot be a factor in explaining the dramatic effect on the rate of change of the mechanical properties resulting in

shorter gel times as a function of r . However, the total amount of silane consumed per unit of time increases with increasing initial silane concentration. Integrating eqn (7) from an initial state to some time t yields (first order reaction)

$$[\text{SiH}] = [\text{SiH}]_0 e^{-\bar{k}t} \quad (18)$$

The extent of reaction, $p(t)$, as a function of silane concentration is given by eqn (6) and is therefore not affected by the initial concentration of silane. The decrease in the gel time with increasing initial silane concentration, i.e. stoichiometric ratio, results from the increasing number of crosslinks formed at the same extent of reaction because of the increasing amount of silane consumed at this extent of reaction.

The second case involved keeping the stoichiometric ratio constant while changing the functionality of the precursor. It should be noted here that in this case the initial silane concentration *and* the vinyl concentration are inherently constant. This can be explained as follows: the density of PBD is independent of molecular weight and the randomly distributed vinyl unit content on the chain is approximately the same for all precursor molecular weights at 8 mole%, and hence the moles of vinyl units per cm^3 is the same for all precursor molecular weights. However, we still observed a dramatic decrease in the gel time as the value of f increased. With increasing precursor chain length the gel point is reached at smaller extent of reactions because fewer chain connections are necessary to achieve a sample spanning network.

This investigation clearly shows that monitoring kinetic evolution of crosslinking reactions by mechanical or chemical means can yield vastly different information. In the simplest case of first order reactions using varying initial compositions, the rate of conversion is not affected while the rate of evolution of mechanical properties can change drastically. This is because chemical monitoring is a measurement of molecular reaction rate while mechanical measurements probe the connectivity of the entire evolving structure.

7 CONCLUSIONS

The critical gel offers itself as the most appropriate reference state for describing gelation. The main reasons for this choice are the following: (1) The critical gel state is well defined since both the critical gel time and the critical extent of reaction are known from rheometry and FTIR, respectively. (2) The reaction conditions can be held constant in the wider vicinity of the gel point. (3) This choice of reference state allows us to

write a simple first order kinetic relationship for $p(t)$ with the precursor composition and functionality (molecular weight) as parameters.

The gel time was found to agree reasonably well with experimental observations on a crosslinking polybutadiene system with several precursor compositions at various temperatures. The kinetic parameters were evaluated using experimental gel times, stoichiometric ratios, and functionalities of a variety of crosslinking samples. The most important parameter, the rate constant \bar{k} , proved to be a function of temperature and platinum concentration, $\bar{k} = \bar{k}(T, [\text{Pt}])$, but it is independent of molecular weight and stoichiometric ratio.

The rate of change of mechanical properties was controlled by the rate of reaction (as a function of temperature and catalyst concentration) and by the precursor composition (functionality and stoichiometry). Mechanical and chemical observations of the crosslinking reaction led to vastly different information since chemistry concerns the reaction rate and mechanics probes the connectivity of the evolving structure.

The rate of the specific crosslinking reaction (hydrosilation) for our system only depends on the concentrations of silane groups and platinum catalyst. The concentration of vinyl groups which varies during the reaction does not influence the rate of reaction, only the initial vinyl concentration enters the picture via the stoichiometric ratios. This independence from one reactant concentration does not necessarily hold for different reacting systems. Hence, additions to our kinetic model might be needed to describe such crosslinking systems.

ACKNOWLEDGEMENTS

This work was supported by the National Science Foundation through the Materials Research Science and Engineering Center (MRSEC) at the University of Massachusetts. One of us (M. M.) is grateful to the German Academic Exchange Service (DAAD-Doktorandenstipendium aus Mitteln des zweiten Hochschulsonderprogramms) for financial support. FTIR measurements were performed in the laboratory of Prof. S. L. Hsu at UMass.

REFERENCES

1. Mussatti, F. G. & Macosko, C. W., Rheology of network forming systems. *Polym. Eng. Sci.*, **13** (1973) 236-240.
2. Gonzalez-Romero, V. M. & Macosko, C. W., Viscosity rise during free

- radical crosslinking polymerization with inhibition. *J. Rheol.*, **29** (1985) 259–272.
3. Macosko, C. W., Rheological changes during crosslinking. *Brit. Polym. J.*, **17** (1985) 239–245.
 4. Macosko, C. W. & Lee, L. J., Heat transfer and property development in liquid siloxane rubber molding. *Rubber Chem. Technol.*, **58** (1985) 436–498.
 5. Bidstrup, S. A. & Macosko, C. W., Chemorheology relations for epoxy-amine crosslinking. *J. Polym. Sci. B, Polym. Phys.*, **28** (1990) 691–707.
 6. Adam, M., Delsanti, M. & Durand, D., Mechanical measurements in the reaction bath during the polycondensation reaction, near the gelation threshold. *Macromolecules*, **18** (1985) 2285–2290.
 7. Tung, C. Y. M. & Dynes, P. J., Relationship between viscoelastic properties and gelation in thermosetting systems. *J. Appl. Polym. Sci.*, **27** (1982) 569–574.
 8. Chambon, F. & Winter, H. H., Stopping of the crosslinking reaction in a PDMS polymer at the gel point. *Polym. Bull.*, **13** (1985) 499–503.
 9. Holly, E. E., Venkataraman, S. K., Chambon, F. & Winter, H. H., Fourier transform mechanical spectroscopy of viscoelastic materials with transient structure. *J. Non-Newtonian Fluid Mech.*, **27** (1988) 17–26.
 10. Venkataraman, S. K., Coyne, L., Chambon, F., Gottlieb, M. & Winter, H. H., Critical extent of reaction of a polydimethylsiloxane network. *Polymer*, **30** (1989) 2222–2226.
 11. Ishida, H. & Smith, M. E., Evolution of the rheological properties during the reactive processing of thermoplastic/thermoset epoxy. *Rheol. Acta*, **30** (1991) 184–196.
 12. Muller, R., Gérard, E., Dugand, P., Rempp, P. & Gnanou, Y., Rheological characterization of the gel point: a new interpretation. *Macromolecules*, **24** (1991) 1321–1326.
 13. Scanlan, J. C. & Winter, H. H., The evolution of linear viscoelasticity near the gel point of end-linking poly(dimethylsiloxane)s. *Makromol Chem., Macromol. Symp.*, **45** (1991) 11–21.
 14. In, M. & Prud'homme, R. K., Fourier transform mechanical spectroscopy of the sol-gel transition in zirconium alkoxide ceramic gels. *Rheol. Acta*, **32** (1993) 556–565.
 15. Arellano, M., Casillas, N. & Gonzalez-Romero, V., Curing of epoxy resins with aliphatic amines: effect of functionality and stoichiometric imbalance, *ANTEC Conf. Proc.*, 1988, pp. 1069–1074.
 16. Batch, G. L., Macosko, C. W. & Kemp, D. N., Reaction kinetics and injection molding of liquid silicone rubber. *Rubber Chem. Technol.*, **64** (1991) 218–233.
 17. Winter, H. H. & Chambon, F., Analysis of linear viscoelasticity of a crosslinking polymer at the gel point. *J. Rheol.*, **30** (1986) 367–382.
 18. Chambon, F. & Winter, H. H., Linear viscoelasticity at the gel point of a crosslinking PDMS with imbalanced stoichiometry. *J. Rheol.*, **31** (1987) 683–697.
 19. Mours, M. & Winter, H. H., Time-resolved rheometry. *Rheol. Acta*, **33** (1994) 385–397.
 20. Flory, P. J., Molecular size distribution in three dimensional polymers: I. Gelation. *J. Am. Chem. Soc.*, **63** (1941) 3083–3090.

21. Flory, P. J., *Principles of Polymer Chemistry*. Cornell University Press, Ithaca, NY, 1953.
22. Stockmayer, W. H., Theory of molecular size distribution and gel formation in branched-chain polymers. *J. Chem. Phys.*, **11** (1943) 45.
23. Gordon, M. & Torkington, J. A., Scrutiny of the critical exponent paradigm, as exemplified by gelation. *Pure Appl. Chem.*, **53** (1981) 1461–1478.
24. Martin, J. E. & Adolf, D., The sol-gel transition in chemical gels. *Ann. Rev. Phys. Chem.*, **42** (1991) 311–339.
25. Stauffer, D., *Introduction to Percolation Theory*. Taylor and Francis, Philadelphia, PA, 1985.
26. Baumgärtel, M., De Rosa, M. E., Winter, H. H., Machado, J. & Masse, M., The relaxation time spectrum of nearly monodisperse polybutadiene melts. *Rheol. Acta*, **31** (1992) 75–82.
27. Aranguren, M. I. & Macosko, C. W., Modulus of polybutadiene networks made by hydrosilation cross-linking. *Macromolecules*, **21** (1988) 2484–2491.
28. De Rosa, M. E. & Winter, H. H., The effect of entanglements on the rheological behavior of polybutadiene critical gels. *Rheol. Acta*, **33** (1994) 220–237.
29. Friedmann, G. & Brossas, J., Synthesis of statistical networks from liquid polybutadienes—IV. *Eur. Polym. J.*, **20** (1984) 1151–1153.
30. Odian, G., *Principles of Polymerization*, 2nd edn. John Wiley, New York, 1981.
31. Miller, D. R., Vallés, E. R. & Macosko, C. W., Calculation of molecular parameters for stepwise polyfunctional polymerization. *Polym. Engng Sci.*, **19** (1979) 272–283.
32. Izuka, A., Winter, H. H. & Hashimoto, T., Molecular weight dependence of viscoelasticity of polycaprolactone critical gels. *Macromolecules*, **25** (1992) 2422–2428.
33. De Rosa, M. E. & Winter, H. H., Determination of the gel point of highly entangled polymers of high molecular weight. *ANTEC Conf. Proc.*, **3** (1993) 2620–2626.
34. Fischer, A. & Gottlieb, M., Side reactions in the endlinking of PDMS networks. *Proc. Networks 86*, Elsinor, Denmark, August 1986.
35. Chalk, A. J. & Harrod, J. F., Homogeneous catalysis: II. The mechanism of the hydrosilation of olefins catalyzed by group VIII metal complexes. *J. Am. Chem. Soc.*, **87** (1965) 16–21.
36. Miron, J., Bhatt, P. & Skeist, I., Silane-modified polybutadienes. In *Recent Advances in Adhesion*. Gordon and Breach, London, 1973, pp. 309–315.
37. Valles, E. M. & Macosko, C. W., The effect of network structure in the equation of rubber elasticity. *Rubber Chem. Technol.*, **49** (1976) 1232–1237.
38. Friedmann, G. & Brossas, J., Synthesis of statistical networks with liquid polybutadiene and telechelic bishydrogenosilyl coupling agents. *Polym. Prepr.*, **26** (1985) 268–269.
39. Colthup, N. B., Daly, L. H. & Wilberley, S. E., *Introduction to Infrared and Raman Spectroscopy*, 3rd edn. Academic Press, Boston, MA, 1990.
40. Noggle, J. H., *Physical Chemistry*. Little, Brown, Boston, MA, 1985.
41. Soltero, J. & Gonzalez-Romero, V., Kinetic study of the curing of poly(dimethylsiloxane) with polyfunctional silanes using temperature programmed IR. *ANTEC Conf. Proc.*, 1988, pp. 1057–1061.

APPENDIX

The simple relationships between gel time, precursor composition, and functionality, eqns (15) and (16), can also be deduced for non-first order kinetics which might apply to different reacting systems.

Introducing the definition of extent of reaction, eqn (6), into the general rate equation, eqn (8), leads to

$$\frac{dp}{dt} = \bar{k}[\text{SiH}]_0^{m-1}(1-p)^m \quad (\text{A1})$$

For first order kinetics, $m = 1$. This results in the simple relationship between p and t , eqn (15), and the new equation for the gel time m as a function of r and f , eqn (16). The corresponding relationships kinetics of order 1.5 and 2 are:

$$m = 1.5: p = 1 - \left(\frac{\sqrt{1 - \frac{1}{\sqrt{r(f-1)}}}}{1 + 0.5\bar{k}[\text{SiH}]_0^{0.5} \sqrt{1 - \frac{1}{\sqrt{r(f-1)}}} (t - t_c)} \right)^2 \quad (\text{A2})$$

$$t_c - t = \frac{2}{\bar{k}[\text{SiH}]_0^{0.5}} \left(\frac{1}{\sqrt{1 - \frac{1}{\sqrt{r(f-1)}}}} - \frac{1}{\sqrt{1-p}} \right) \quad (\text{A3})$$

$$m = 2: p = 1 - \frac{1 - \frac{1}{\sqrt{r(f-1)}}}{1 + \bar{k}[\text{SiH}]_0 \left(1 - \frac{1}{\sqrt{r(f-1)}}\right) (t - t_c)} \quad (\text{A4})$$

$$t_c - t = \frac{1}{\bar{k}[\text{SiH}]_0} \left(\frac{1}{1 - \frac{1}{\sqrt{r(f-1)}}} - \frac{1}{1-p} \right) \quad (\text{A5})$$

These equations are somewhat more complex than eqns (15) and (16) because the initial silane concentration $[\text{SiH}]_0$ is an additional parameter that influences the gel time. In case of first order kinetics, only the ratio of initial silane to initial vinyl concentration (stoichiometric ratio r) is important.